npg

Acquisition of epithelial–mesenchymal transition and cancer stem cell phenotypes is associated with activation of the PI3K/Akt/mTOR pathway in prostate cancer radioresistance

L Chang[1,2], PH Graham[1,2], J Hao[1,2], J Ni[1,2], J Bucci[1,2], PJ Cozzi[1,2,3], JH Kearsley[1,2] and Y Li*[1,2]

Radioresistance is a major challenge in prostate cancer (CaP) radiotherapy (RT). In this study, we investigated the role and association of epithelial–mesenchymal transition (EMT), cancer stem cells (CSCs) and the PI3K/Akt/mTOR signaling pathway in CaP radioresistance. We developed three novel CaP radioresistant (RR) cell lines (PC-3RR, DU145RR and LNCaPRR) by radiation treatment and confirmed their radioresistance using a clonogenic survival assay. Compared with untreated CaP-control cells, the CaP-RR cells had increased colony formation, invasion ability and spheroid formation capability ($P < 0.05$). In addition, enhanced EMT/CSC phenotypes and activation of the checkpoint proteins (Chk1 and Chk2) and the PI3K/Akt/mTOR signaling pathway proteins were also found in CaP-RR cells using immunofluorescence, western blotting and quantitative real-time PCR (qRT-PCR). Furthermore, combination of a dual PI3K/mTOR inhibitor (BEZ235) with RT effectively increased radiosensitivity and induced more apoptosis in CaP-RR cells, concomitantly correlated with the reduced expression of EMT/CSC markers and the PI3K/Akt/mTOR signaling pathway proteins compared with RT alone. Our findings indicate that CaP radioresistance is associated with EMT and enhanced CSC phenotypes via activation of the PI3K/Akt/mTOR signaling pathway, and that the combination of BEZ235 with RT is a promising modality to overcome radioresistance in the treatment of CaP. This combination approach warrants future in vivo animal study and clinical trials.

Prostate cancer (CaP) remains a significant medical burden in developed countries and accounts for an estimated 94 000 deaths in Europe in 2008 and 33 720 in the United States in 2011.[1] Around 70% of these patients present with organ-confined disease, with the majority presenting with low- or intermediate-risk CaP.[2] Radical prostatectomy (RP) and radiation therapy (RT) including external-beam radiotherapy (EBRT), and brachytherapy are the three main treatment options for localized CaP. Although these primary therapies are associated with high-cancer control rates for localized disease, up to a third of patients undergoing these therapies will have a biochemical recurrence (BCR) after local therapy.[3]

Efforts to improve the outcome after EBRT for CaP patients have focused on delivering a higher dose to the tumor. Eade et al.[4] recommended doses of ≥ 80 Gy for most men with CaP due to significant benefit for treatment outcome. Further dose escalation to 82 Gy in an American College of Radiology 03–12 phase II trial yielded significant acute and late morbidity.[5]

There is a concern that further dose increases may lead to more toxicity. Radiation sensitivity has the potential to influence the efficacy of RT, and CaP is the leading radioresistant (RR) malignancy currently.[6] Investigating the mechanisms of radioresistance and associated signaling pathways is urgent and important for the effect of RT in CaP.

Emerging evidence suggests that epithelial–mesenchymal transition (EMT) has a crucial role in cancer radiation resistance.[7] EMT is characterized by the loss of adhesion, negative expression of E-cadherin and enhanced cell motility as well as the acquisition of mesenchymal characteristics, such as expression of vimentin and myosin and invasive motility.[8] EMT was first recognized as a feature of embryogenesis and important for morphogenesis during embryonic development.[9] In addition, inducing EMT in tumor cells not only encourages tumor cell invasion and metastasis but also results in chemo-/radioresistance.[10–12] Although the relationship of EMT with cancer metastasis has only been recently reviewed,[13] the role of EMT in CaP radioresistance remains elusive.

[1]Cancer Care Centre and Prostate Cancer Institute, St. George Hospital, Gray St. Kogarah, Sydney, New South Wales 2217, Australia; [2]St. George Clinical School, Faculty of Medicine, University of New South Wales, Kensington, New South Wales 2052, Australia and [3]Department of Surgery, St. George Hospital, Sydney, New South Wales 2217, Australia
*Corresponding author: Y Li, Cancer Care Centre and Prostate Cancer Institute, St. George Hospital, Gray St. Kogarah, Sydney, New South Wales 2217, Australia. Tel: +61-2-9113 2514; Fax: +61-2-9113 4048; E-mail: y.li@unsw.edu.au

2

Recently, the cancer stem cell (CSC) theory has offered a potential explanation for the relapse and resistance that occurs in many tumors after therapy. The theory hypothesizes that tumors contain heterogeneous cell populations and that tumor growth is driven by a discrete subpopulation of cells (CSCs). CSCs (also called tumor-initiating cells) may produce tumors through the stem cell processes of self-renewal and differentiation into multiple cell types. These CSCs can provide a reservoir of cells that cause tumor recurrence even after therapy.[9] The CSC model has gained increasing attention and CSCs have the potential to resist RT and chemotherapy, reducing effectivity of therapy.[14] Bao et al.[15] showed that CD133^{+} glioblastomas CSCs are more resistant to RT than non-CSCs. In a recent study, we also demonstrated that CD44 is a CSC biomarker associated with radioresistance in CaP cells.[16] Investigation of the relationship between the radioresistance of cancer and CSCs is potentially useful for predicting radioresistance of cancers and developing more effective and specific radiosensitizers. However, the role of CSCs, their relationship with EMT and the regulation of signaling pathways in CaP radioresistance are still unclear.

In this study, we hypothesized that EMT and CSCs are involved in CaP radiation resistance and correlated with the PI3K/Akt/mTOR singaling pathway; specifically blocking the PI3K/Akt/mTOR signaling pathway proteins as such may affect EMT/CSC phenotypes and improve CaP radiosensitivity. We found that the EMT and enhanced CSC phenotypes are associated with CaP radioresistance via activation of the PI3K/Akt/mTOR signaling pathway. Using a dual PI3K/mTOR inhibitor BEZ235 (targeting both PI3K and mTOR) combined with RT markedly reduced EMT/CSC phenotypes and increased CaP radiosensitivity, as well as induced increased apoptosis in CaP-RR cells. We suggest that this combination approach (BEZ235 and RT) holds promise for future CaP radiotherapy.

Results

Establishment of CaP-RR cell lines. To generate CaP-RR cell lines, PC-3, DU145 and LNCaP CaP cell lines were treated with different dosages (2, 4, 6 and 8 Gy) of radiation for five consecutive days. Our results indicated that the 2 Gy/per day for five consecutive days was the maximum tolerance dose for all three CaP cell lines. The significant morphological changes in RT-treated cells include loss of the glandular morphology, vacuolated cytoplasm, pleomorphic nuclei and enlarged cell size when compared with control CaP cells (Supplementary Figure S1).

Validation of radioresistance in three CaP-RR cell lines. To confirm radioresistance in three radiation-treated CaP cell lines, CaP-RR and CaP-control cells were exposed to a range of single radiation doses (2–10 Gy) and were examined using the clonogenic survival assay. The survival fractions in CaP-RR cells were significantly higher along with increasing dosage compared with CaP-control cells (Figure 1a). Colony formation was increased for CaP-RR cells (Supplementary Figure S2). The colony numbers in CaP-RR cells had 2- to 42-fold increase compared with those

in CaP-control cells ($P < 0.05$) (Supplementary Figure S2). The typical images for colony formation in different doses of RT in CaP-RR and control cells are shown in Figure 1b. These data suggest that CaP-RR cell lines produced in this study are RR cells, which can be used in the following functional studies.

CaP-RR cells increase cell invasion and sphere formation capability. Cell invasion in CaP-RR cells was much higher in three CaP-RR cell lines compared with three CaP-control cell lines ($P < 0.05$) (Figure 2a). The average percentage of invasion rate for PC-3RR, DU145RR and LNCaPRR was 75%, 62%, 85%, respectively, whereas the average percentage of invasion rate for PC-3, DU145 and LNCaP was 35%, 35%, 42%, respectively. Among three CaP cell lines, the most significant difference in invasion ability was found between LNCaPRR and LNCaP-control cells ($P < 0.0001$) (Figure 2a). Representative images for the invasion ability from each cell line are shown in Figure 2b. Sphere formation in CaP-RR cells was also increased in three CaP-RR cell lines compared with three CaP-control cell lines ($P < 0.01$) (Figure 2c). The highest sphere formation among three CaP-RR cell lines was DU145RR cells ($P < 0.001$). Typical images for the comparison of the sphere formation between CaP-RR cells and CaP-control cells are shown in Figure 2d.

EMT phenotypic expression in CaP-RR cells. Three CaP-RR cell lines consistently showed the downregulation of epithelial marker E-cadherin and upregulation of mesenchymal markers including N-cadherin, Vimentin, OCT3/4, SOX2 and alpha smooth muscle actin (αSMA) compared with CaP-control cells by confocal microscope (Figure 3a). The binding sites of these EMT markers are both membrane and cytoplasm. No detectable staining was seen in the cells incubated with negative controls (data not shown). The immunofluorescence staining results for EMT markers in different CaP cell lines are summarized in Supplementary Table S1. The results from western blotting (Figure 3b) and quantitative real-time PCR (qRT-PCR) in mRNA levels (Figure 3c) were consistent with those from the immunofluorescence.

Enhanced CSC phenotypes in CaP-RR cells. To determine whether a population of CSCs is involved in CaP radioresistance, we measured the expression of several putative CSC markers including CD44, CD44v6, CD326 and ALDH1 as well as the stem-related transcription factors-Nanog and Snail. Three CaP-RR cell lines also demonstrated enhanced expression of these CSC markers compared with three CaP-control cell lines by confocal microscope (Figure 4a). The binding sites of these CSC markers are either membrane or cytoplasm or both. No detectable staining was seen in the cells in negative controls (data not shown). The immunofluorescence staining results for these CSC markers in different CaP cell lines are summarized in Supplementary Table S2. The results from western blotting (Figure 4b) and qRT-PCR in mRNA levels (Figure 4c) were consistent with the results from immunofluorescence.
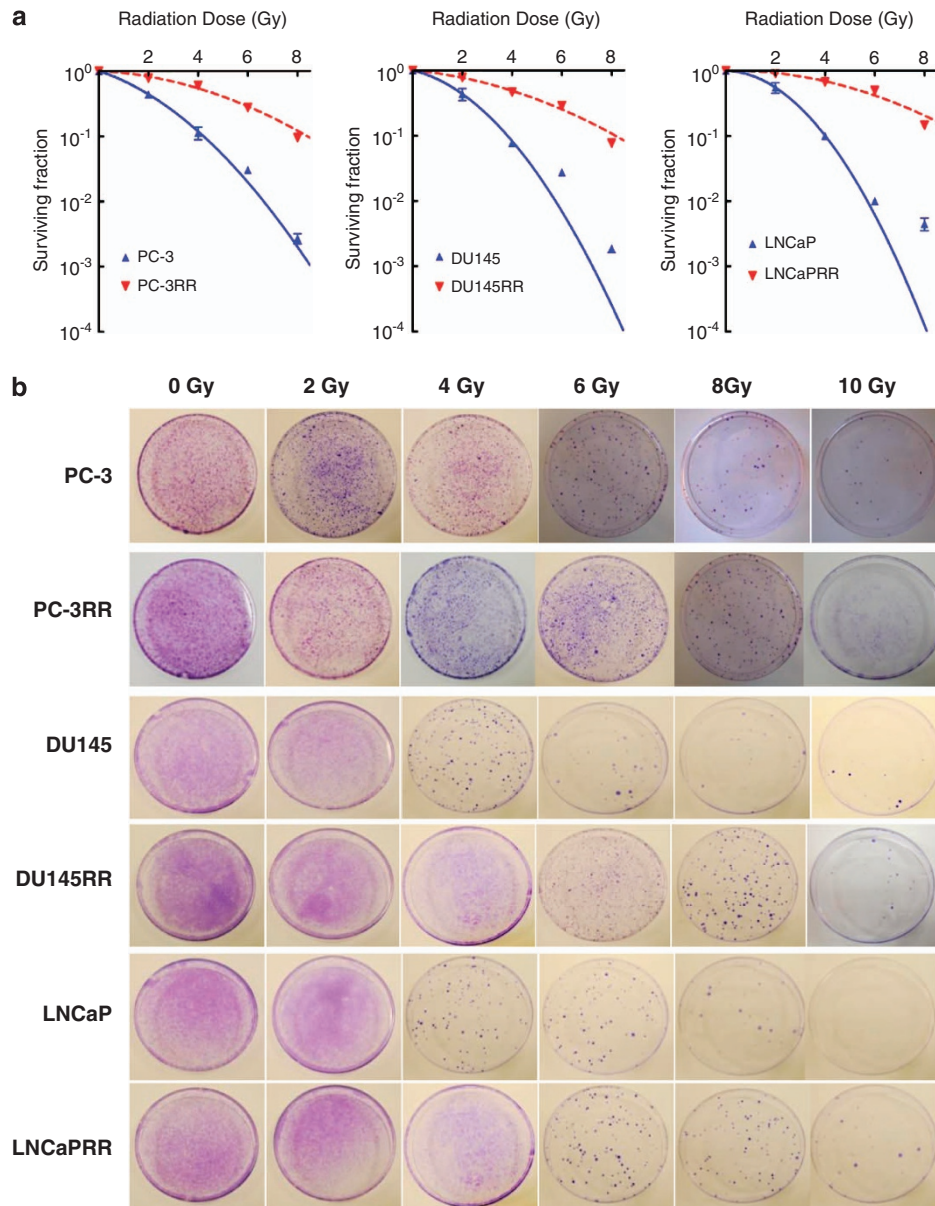
Figure 1 Different radiosensitivity to RT in CaP-RR and CaP-control cells. CaP-RR and CaP-control cells were seeded in 10 cm dishes and treated with 2–10 Gy radiation. The colonies that formed after 10–12 d incubation were counted to calculate the survival fractions. (a) Survival fractions in CaP-RR cells (PC-3RR, DU145RR and LNCaPRR) were significantly increased compared with those in CaP-control cells ($P < 0.01$). (b) Typical images are shown for colony growth in CaP-RR and CaP-control cells after exposure to different radiation doses. Images were taken using a Sony camera (Tokyo, Japan). All data used in RR cell lines were based on cells between 5 and 6 weeks post radiation treatment. All results were from three independent experiments (Mean ± S.D., $n = 3$)

Checkpoint proteins are activated in CaP-RR cells. To examine whether checkpoint proteins were involved in CaP radioresistance, checkpoint proteins t-Chk1/p-Chk1 and t-Chk2/p-Chk2 were examined by western blotting. Our results showed that the expression of p-Chk1 and p-Chk2 was increased in CaP-RR (PC-3RR, DU145RR and LNCaPRR) cells compared with that in CaP-control cells, whereas no change was found in t-Chk1 and t-Chk2 expression between CaP-RR and CaP-control cells (Figure 5a), which indicated that checkpoint proteins (p-Chk1 and p-Chk2) are activated in CaP-RR cells and associated with CaP radioresistance.

PI3K/Akt/mTOR signaling pathway is activated in CaP-RR cells. To investigate whether the PI3K/Akt/mTOR signaling pathway is involved in CaP radio-resistance, we examined the expression of t-Akt/p-Akt, t-mTOR/p-mTOR, t-S6K/p-S6K and t-4EBP1/p-4EBP1 using western blotting analysis. Our results indicated that increased p-Akt, p-mTOR, p-S6K and p-4EBP1 levels were found in CaP-RR (PC-3RR, DU145RR and LNCaPRR) cells, whereas no change was found in t-Akt, t-mTOR, t-S6K and t-4EBP1 (Figure 5a), suggesting that the PI3K/Akt/mTOR signaling pathway is activated in CaP resistance.
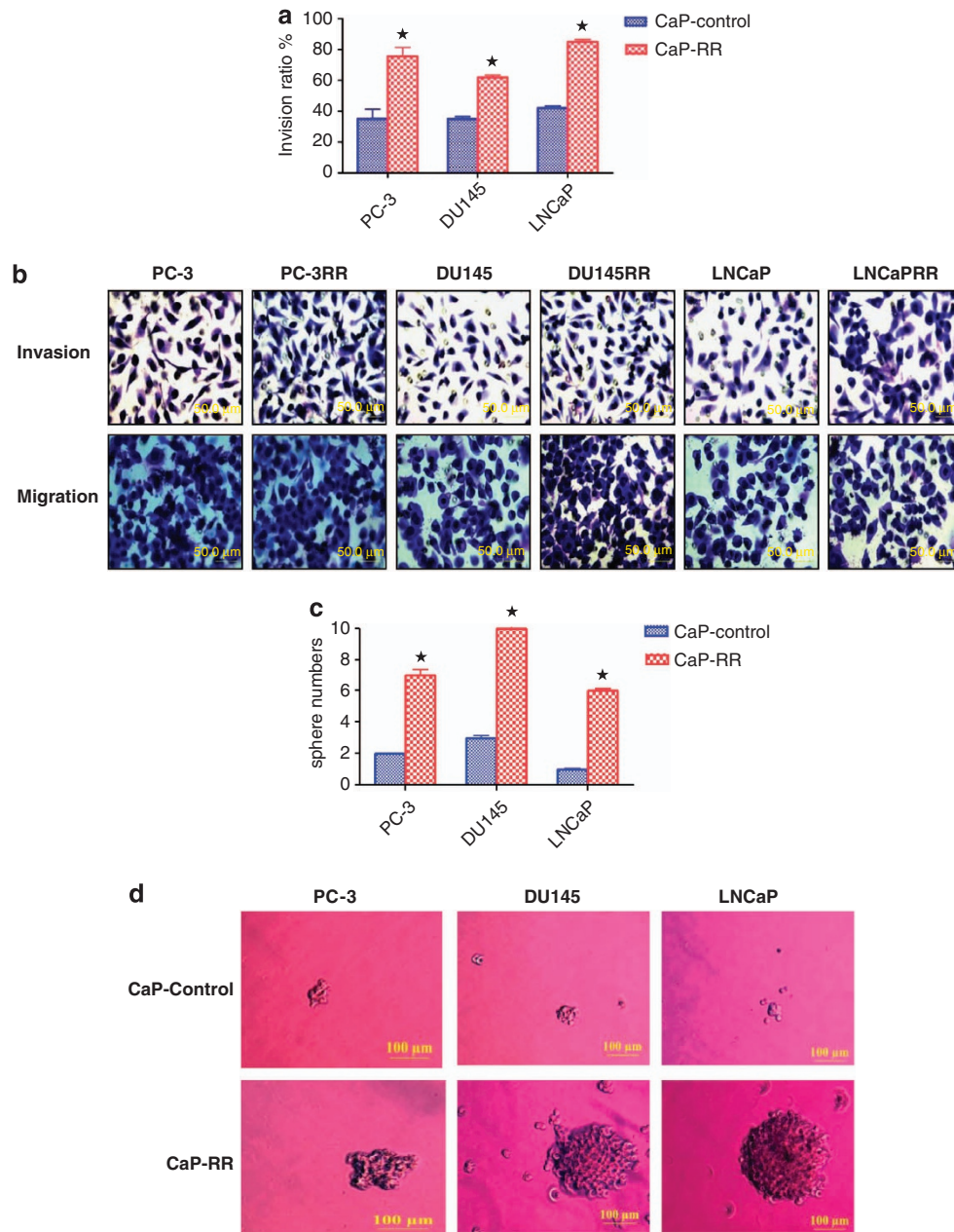
Figure 2 Matrigel invasion and spheroid formation in CaP-RR and CaP-control cells. (a) The cells were incubated 12 h for the invasion assay. The invasive potential in CaP-RR cells was significantly increased in PC-3RR, DU145RR and LNCaPRR cells compared with CaP-control cells (★ , $P < 0.01$). (b) Representative images for CaP cell invasion and migration in CaP-RR and CaP-control cells are shown. Magnification: $\times 200$ in all images. (c) The spheroid formation ability in CaP-RR cells was significantly enhanced compared with CaP-control cells (★ , $P < 0.01$) after 5 days culture. (d) Representative images for spheroid formation in CaP-RR cells and CaP-control cells are shown. The upper images are from CaP-control cells (cell numbers < 50/spheroid), whereas the lower images were from CaP-RR cells (cell numbers > 50/spheroid). All data used in RR cell lines were based on cells between 5 and 6 weeks post radiation treatment. All results were from three independent experiments (Mean $\pm$ S.D., $n = 3$)

A dual PI3K/mTOR inhibitor BEZ235 affects the expression PI3K/Akt/mTOR signaling proteins and EMT/CSC phenotypes. The IC_{50} values of BEZ235 on three CaP-RR and CaP-control cell lines as well as normal prostate RWPE-1 cell line (control) were evaluated using MTT assay for the combination treatment with radiation. We found all IC_{50} values from CaP-RR cells are higher than those from CaP-control cells at all time points (Supplementary Table S3), further confirming the resistant property after RT. Interestingly, we also found that the IC_{50} values in RWPE-1 cell line are much higher than in CaP-RR- and CaP-control cell lines (3- to 16-fold) at all time points (Supplementary Table S3), suggesting that normal prostate cells are not sensitive to BEZ235 treatment, and BEZ235 is promising in future *in vivo* study and clinical trials. The IC_{50} values for BEZ235 in CaP-RR, CaP-control cells and normal prostate RWPE-1 cells are summarized in Supplementary Table S3. At 48 h incubation, the most sensitive CaP-RR cell line is DU145RR cell line (72.6 nM). We chose ½ IC_{50} value for our combination study, which is based on our previous similar study.[17]
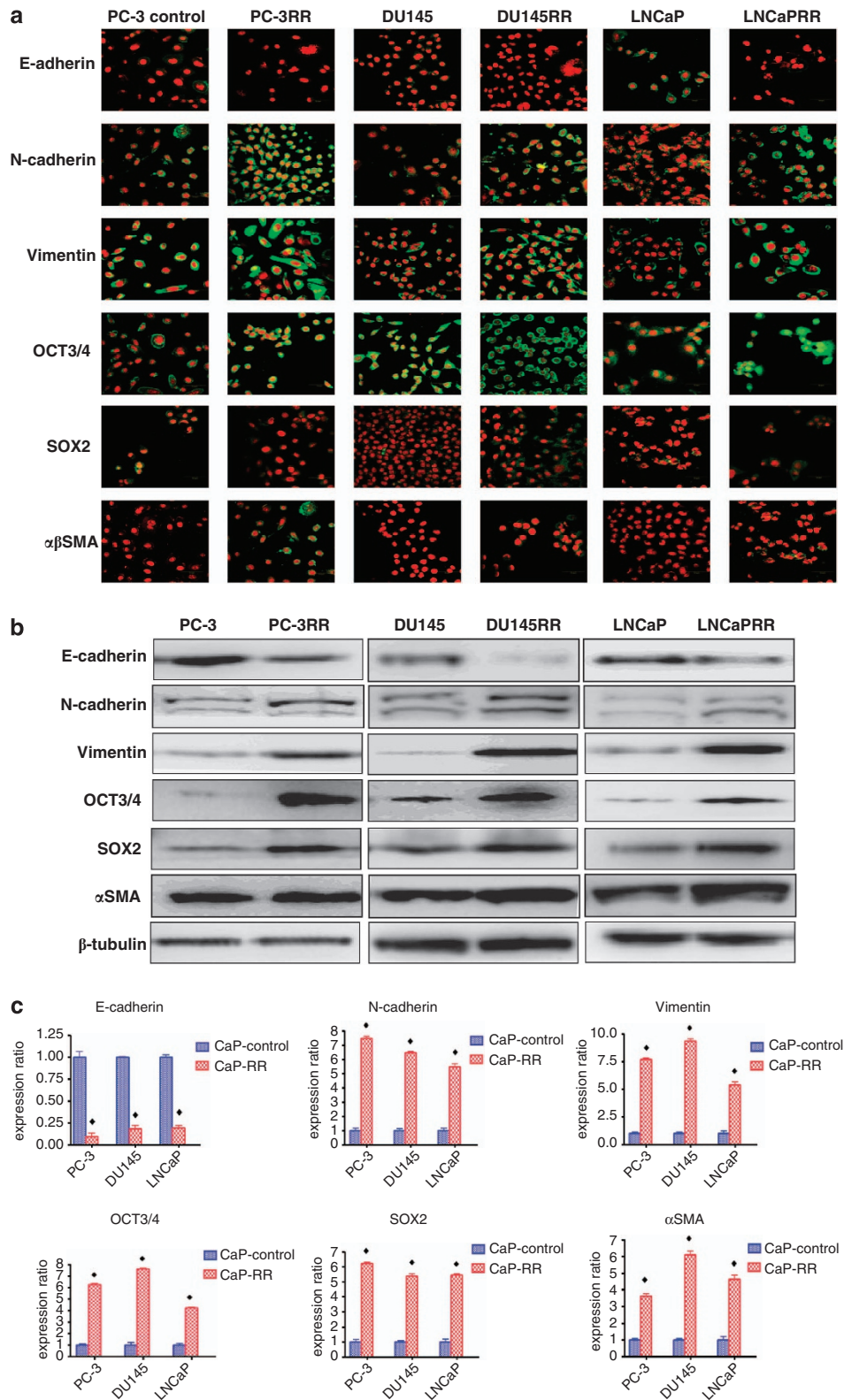
Figure 3 EMT phenotypic expression in CaP-RR and CaP-control cells. Reduced expression of membranous E-cadherin and increased membranous or cytoplasmic expression of N-cadherin, Vimentin, OCT3/4, SOX2 and αSMA were found in CaP-RR cells. (a) Representative immunofluorescence images of E-cadherin, N-cadherin, Vimentin, OCT3/4, SOX2 and αSMA (green) are shown for CaP-RR and CaP-control cells. Nuclei are stained with PI (red). Magnification: all images × 400. (b) Western blotting results were consistent with immunofluorescence staining results. β-Tubulin was used as a loading control. (c) Phenotypic changes of EMT markers in CaP-RR cells using immunofluorescence and western blotting were further confirmed by qRT-PCR (♦, $P < 0.01$). All data used in RR cell lines were based on cells between 5 and 6 weeks post radiation treatment
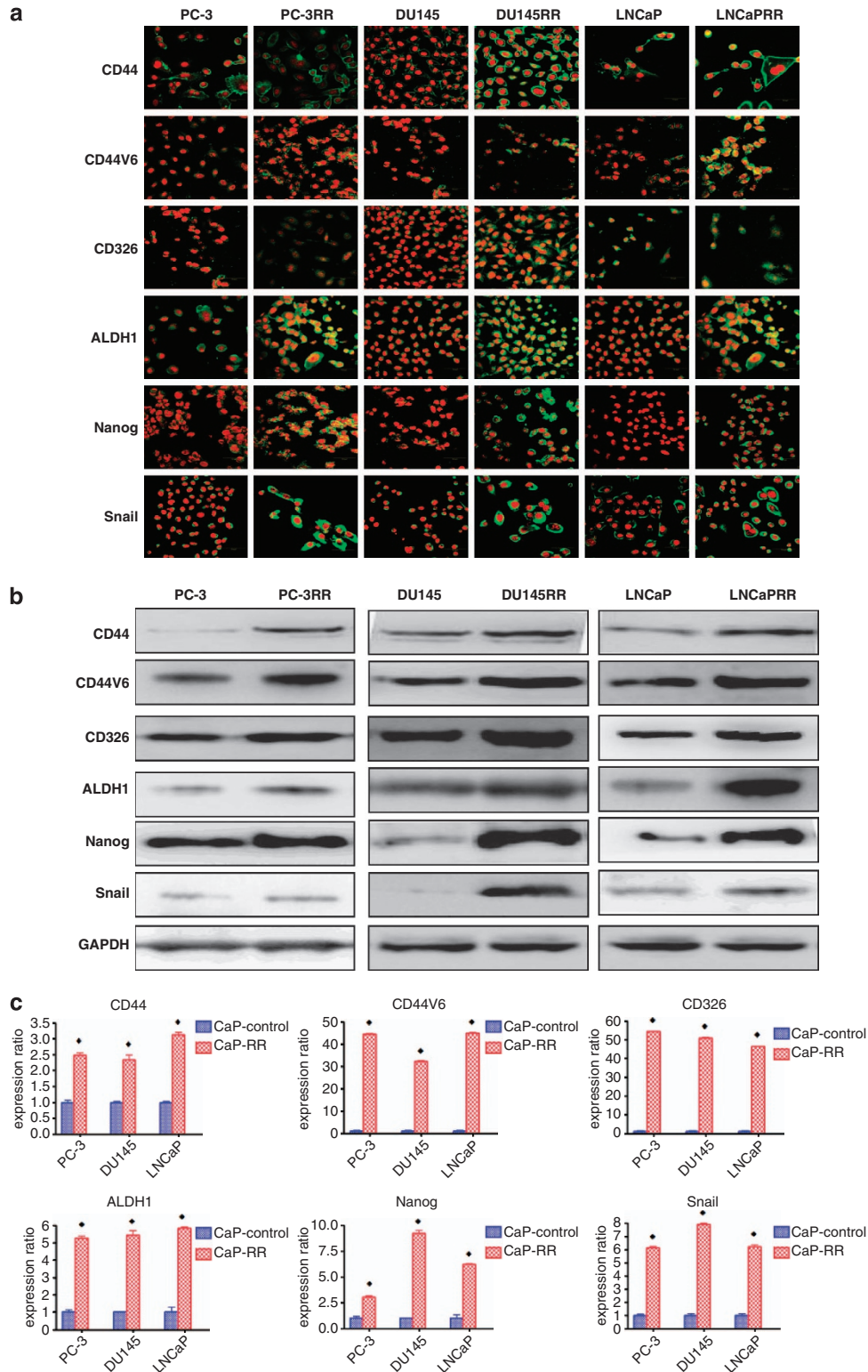
Figure 4 CSC phenotypic expression in CaP-RR and CaP-control cells. The enhanced CSC phenotypes were seen in CaP-RR (PC-3RR, DU145RR and LNCaPRR) cells. (**a**) Representative immunofluorescence images of membranous or cytoplasmic expression of CD44, CD44v6, CD326, ALDH1, Nanog and Snail are shown in CaP-RR and CaP-control cells. Nuclei were stained with PI (red). Magnification × 400 in all images. (**b**) Western blotting results were consistent with the immunofluorescence staining results. GAPDH was used as a loading control. (**c**) The phenotypic changes of CSC in CaP-RR cells were further confirmed by qRT-PCR (◆, $P < 0.01$). All data used in RR cell lines were based on cells between 5 and 6 weeks post radiation treatment. All results were from three independent experiments (Mean ± S.D., $n = 3$)
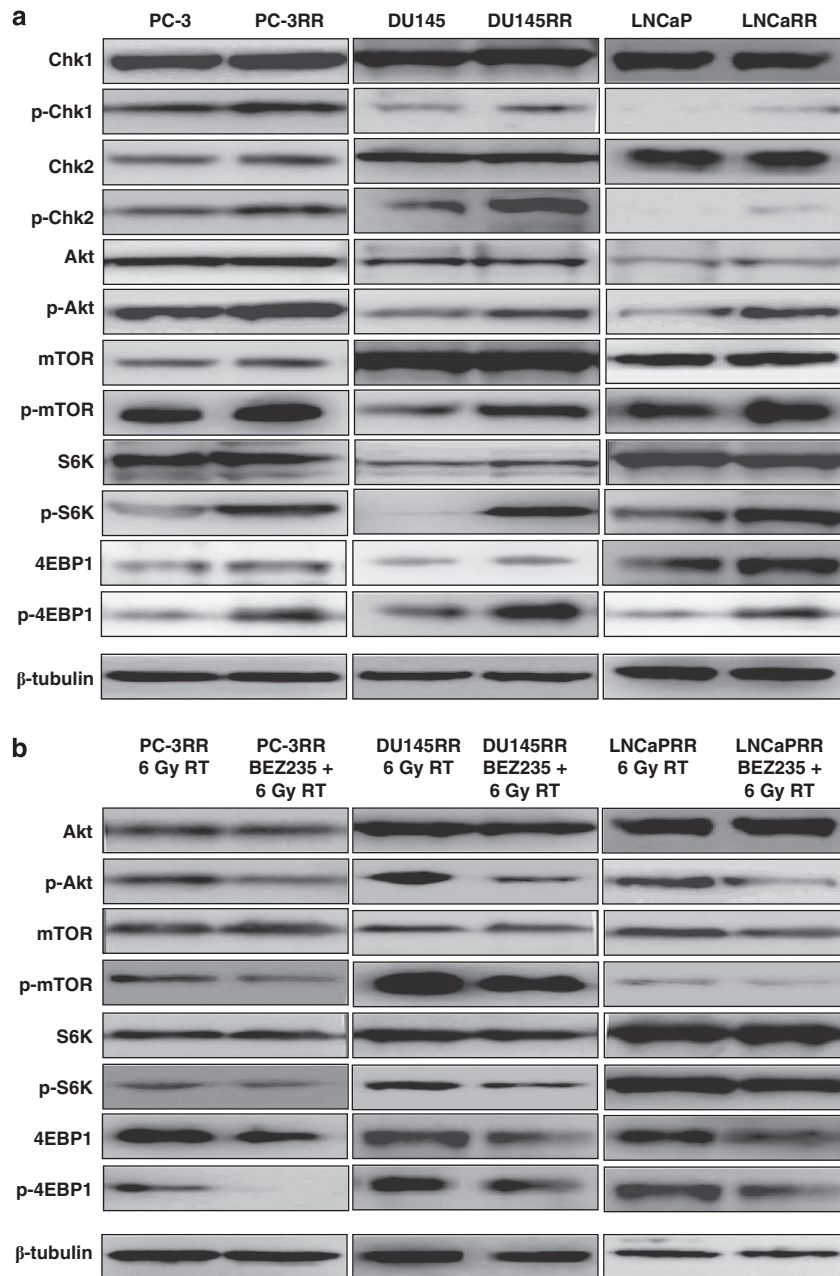
Figure 5 CaP-RR cells activate checkpoint proteins and the PI3K/Akt/mTOR pathway, and the effect of RT and BEZ235 on the expression of PI3K/Akt/mTOR pathway proteins. Two markers (Chk1 and Chk2) involved in radiation checkpoint and eight signal transduction molecules (mTOR, p-mTOR, Akt, p-Akt, 4EBP1, p-4EBP1, S6K and p-S6K) were assessed to investigate the roles of checkpoint proteins or PI3K/Akt/mTOR signaling proteins in CaP radioresistance. (**a**) The levels of p-Chk1 and p-Chk2, p-Akt, p-mTOR, p-S6K and p-4EBP1 were increased in CaP-RR cells compared with CaP-control cells, whereas no change was found in total of Chk1, Chk2, Akt, mTOR, S6K and 4EBP1 proteins in both CaP-RR and control cells. Representative results are shown. (**b**) After 12 h treatment by 6 Gy RT alone or combination treatment with RT and BEZ235 (BEZ235 was used for 12 h prior RT and then 6 Gy was applied. Cell lysate was extracted after RT applied for 12 h). Reduced levels of p-Akt, p-mTOR, p-S6K and p-4EBP1 were detected in CaP-RR cells in combination treatment compared with single 6 Gy treatment. β-Tubulin was used as a loading control. All data used in RR cell lines were based on cells between 5 and 6 weeks post radiation treatment. All data were from three independent experiments (Mean $\pm$ S.D., $n = 3$). p-mTOR: phosphorylated-mTOR; p-Akt: phosphorylated-Akt; p-4EBP1: phosphorylated-4EBP1; p-S6K: phosphorylated-S6K

The expression of p-Akt, p-mTOR, p-S6K, p-4EBP1 and t-4EBP1 in CaP-RR cells treated by combining ½ IC_{50} dose BEZ235 and 6 Gy RT was downregulated compared with that in RT alone, whereas no change was seen for the expression of t-Akt, t-mTOR, t-S6K in all CaP-RR cell lines (Figure 5b). Compared with the RT and combination treatment (BEZ235 + RT), the RR cells without any treatments show

the highest expression of p-Akt, p-mTOR, p-S6K and p-4EBP1 (data not shown). To further investigate the association of the PI3K/Akt/mTOR signaling pathway with EMT and CSC phenotype, the levels of EMT and CSC marker expression were also examined after single RT and combination treatment with ½ IC_{50} dose BEZ235 and 6 Gy radiation. Our results indicated that for EMT markers, E-cadherin

expression was increased and the levels of N-cadherin, Vimentin, OCT3/4, SOX2 and αSMA expression were reduced in CaP-RR cells in combination treatment, whereas for CSC markers, the expression of CD44, CD44v6, CD326, ALDH1, Nanog and Snail was all reduced in CaP-RR cells in combination treatment compared with that in 6 Gy RT alone (Figure 6a). The control RR cells without treatments showed the lowest expression of E-cadherin, and the highest expression of N-cadherin, Vimentin, OCT3/4, SOX2, αSMA CD44, CD44v6, CD326, ALDH1, Nanog and Snail (data not shown). These data indicate that the dual PI3K/mTOR inhibitor BEZ235 affected the PI3K/Akt/mTOR pathway and concomitantly reduced both EMT and CSC phenotypic expression.

Combination therapy with BEZ235 and RT increases radiosensitivity and induces more apoptosis in CaP-RR cells. To investigate the radiosensitivity effect of BEZ235 on three CaP-RR cell lines, single treatment with BEZ235 or RT alone and combination treatment with BEZ235 and RT were performed and compared. After combination treatment by ½ IC_{50} dose BEZ235 and 6 Gy irradiation, three CaP-RR cells consistently showed significant reduction in colony formation, when compared with the cells treated with ½ IC_{50} dose BEZ235 or 6 Gy radiation alone or the untreated CaP-RR control cells ($P < 0.05$) (Figure 6b). Although single BEZ235 or 6 Gy radiation treatment caused the reduction of colony formation in CaP-RR cells compared with the untreated CaP-RR control cells, no significant difference was found between these two single treatments ($P > 0.05$). Among the three combination-treated CaP-RR cell lines, PC-3RR cells are the most radiosensitive cell line and the reduction of colony formation is 86.7%. These findings indicate that the dual PI3K/mTOR inhibitor BEZ235 could increase radiosensitivity of CaP-RR (PC-3RR, DU145RR and LNCaPRR) cells. The typical images for colony formation from different treatments are shown in Figure 6c. In addition, compared with untreated control, BEZ235 or RT alone, combination treatment with BEZ235 and RT induced more apoptotic cells (Figure 6d).

Discussion

Radioresistance continues to be a major problem in the treatment of CaP. The molecular mechanisms underlying CaP radioresistance remain unclear. Identification of the mechanisms and signaling pathways that impact the radiosensitivity will be helpful in finding useful therapeutic targets, developing novel treatment approaches and overcoming recurrence after RT in CaP patients. Using CaP-RR cells and molecular and cell biology approaches, we present novel insight into the mechanisms associated with EMT and enhanced CSC phenotypes and the activation of the PI3K/Akt/mTOR signaling pathway in CaP radioresistance. Our findings are summarized in the model presented in Figure 7.

In this study, we developed three novel CaP-RR (PC-3RR, DU145RR and LNCaPRR) cell lines derived from clones that had survived after irradiation, which represent androgen-responsive (LNCaP) and androgen-nonresponsive (PC-3 and DU145) stages during CaP progression and can appropriately mimic clinical RR condition and metastasis (recurrence) after RT.

We examined the newly established cell lines with respect to growth and sensitivity to a range of ionizing radiation exposure and found that the growth rate was reduced and clonogenic survival was significantly increased in CaP-RR cells after 5 weeks radiation treatment compared with untreated CaP-control cells. Our observations clearly indicated that all three CaP-RR cells are RR and can be used as excellent *in vitro* models to study mechanisms leading to CaP recurrence after radiation treatment.

We conducted invasion and migration studies and found that the invasion/migration ability in CaP-RR cells was increased compared with that in CaP-control cells, suggesting that these RR CaP cells have more potential to metastasize, which is the main reason for clinical cancer recurrence after RT. The sphere culture assay has been proposed as a valuable method for isolating cancer cells with conserved stemness determinants that are able to propagate in defined media.[18] Sphere formation assay best mimics the process of enriching and proliferating of CSCs and is currently considered as a golden *in vitro* model for CSC research. In the current study, we found that all three CaP-RR cell lines can significantly form more spheres in an appropriate cell number compared with the CaP-control cells, indicating that CSCs are closely associated with radioresistance and could be enriched in CaP-RR cells. The remaining RR cells after RT can be a subpopulation of intrinsic resistant cells with CSC characteristics. These enriched CSCs can provide a very good model to mimic clinical condition and study the roles of CSCs in CaP radioresistance.

Recent studies in breast cancer demonstrated that EMT might affect therapeutic resistance,[19] however, in CaP, such studies are far fewer in number, especially in RR field. Here, we first demonstrated that downregulation of E-cadherin and upregulation of N-cadherin, Vimentin, OCT3/4, OCT4, SOX2 and αSMA were found in CaP-RR cells in both protein (immunofluorescence and western blotting) and molecular levels (qRT-PCR) compared with untreated CaP-control cells, indicating that EMT is correlated with CaP radioresistance. The EMT expression is also consistent with the increased invasion/migration in CaP-RR cells, further confirming that EMT is involved in CaP radioresistance and metastasis.

Accumulated data indicate that the induction of EMT enhances self-renewal and the acquisition of CSC characteristics[20,21] and that CSCs- and EMT-related cells share same markers and properties,[21] illustrating a relation between EMT and CSCs. However, the link between CSCs/EMT and CaP radioresistance is still unclear. CD44, CD44v6, CD326 and ALDH1 are putative CaP CSC markers expressed on the cell surface.[22–24] Nanog and Snail are self-renewal proteins as transcription factors in the regulation of CSCs.[25,26] Nanog has been reported to promote CSC characteristics and CaP resistance to androgen deprivation.[27] To the best of our knowledge, the direct link between Snail as a CSC marker in CaP has not been reported so far. In the current study, we first demonstrated that the enhanced expression of CSC-related markers (CD44, CD44v6, CD326, ALDH1, Nanog and Snail) was found in CaP-RR cells compared with untreated CaP cells, suggesting that CSCs are associated with CaP radioresistance. Our recent report also indicated that the downregulation of CD44 using small interfering RNA (siRNA)
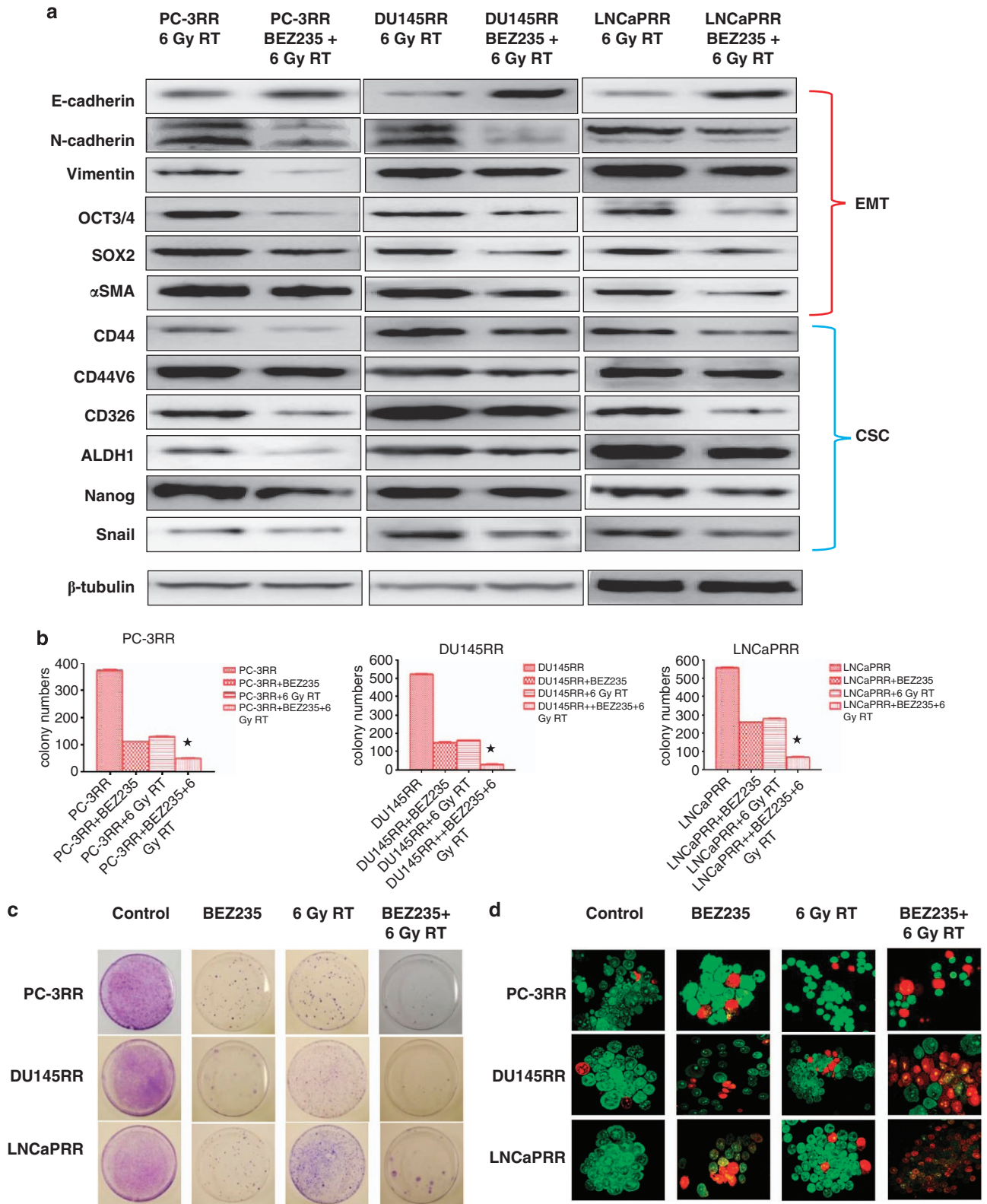
Figure 6 Effect of BEZ235 and RT on the expression of EMT/CSCs and radiosensitivity in CaP-RR cells. Combination treatment with BEZ235 and RT reversed EMT expression and reduced the levels of CSC marker expression in CaP-RR cells compared with the RT alone. (**a**) CaP-RR cells were treated with single RT (6 Gy) for 12 h or combination (BEZ235 was used for 12 h prior RT and then 6 Gy was applied. Cell lysate was extracted 12 h after RT. Typical results for EMT/CSC phenotypic changes after different treatments are shown. β-Tubulin was used as a loading control. (**b**) Colony formation was significantly reduced in combination treatment with BEZ235 and RT compared with single BEZ236, 6 Gy RT alone or vehicle control in CaP-RR cells (★ , $P < 0.01$). (**c**) Typical images of colony growth for the different treatments are shown. (**d**) Combination treatment induced more apoptotic cells in CaP-RR cells compared with single BEZ235 or RT or control. All data used in RR cell lines were based on cells between 5 and 6 weeks post radiation treatment. All data were from three independent experiments ($n = 3$)
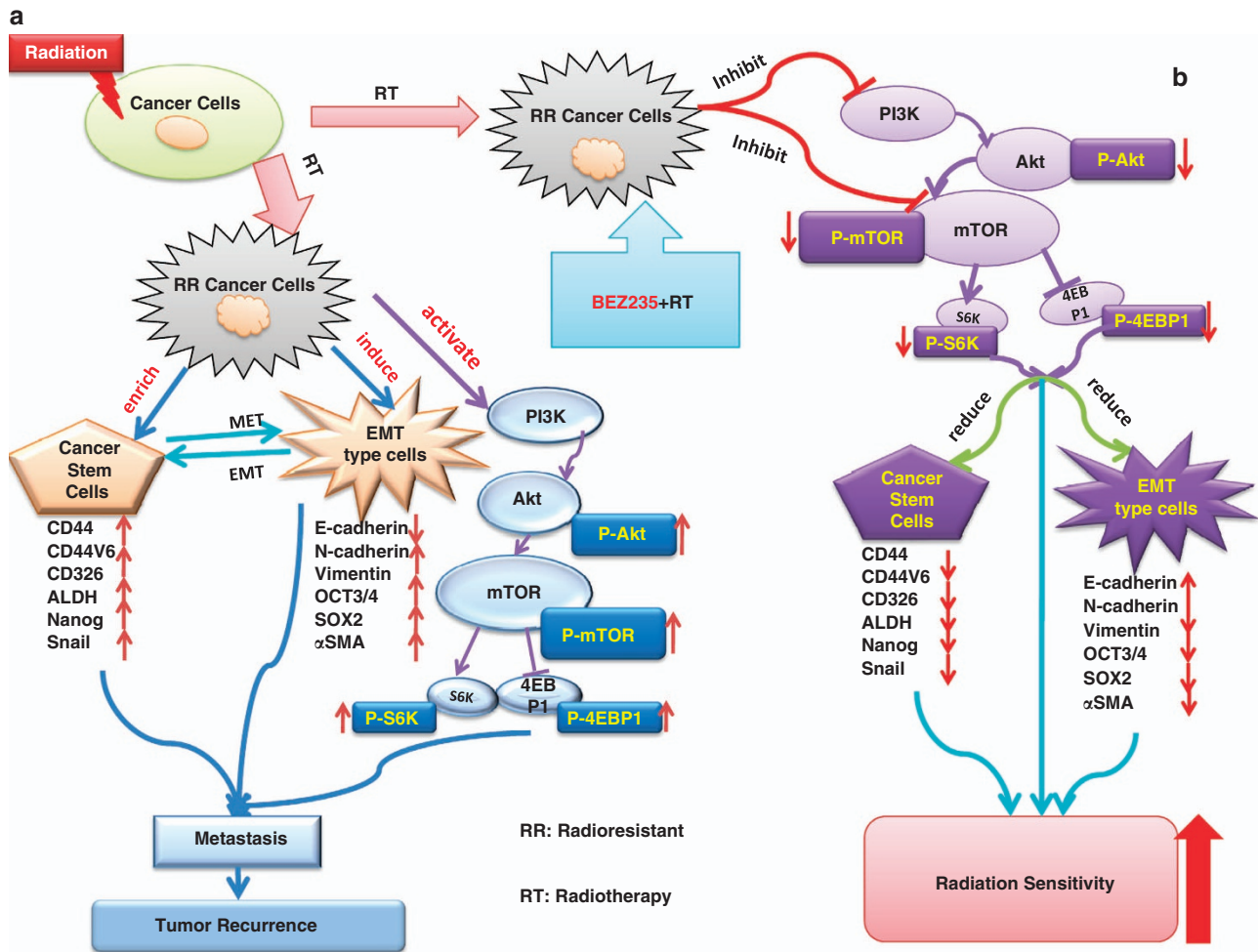
Figure 7 Diagram showing the model proposed for the association of EMT, CSCs and the PI3K/Akt/mTOR signaling pathway in CaP radioresistance and the effect of possible action of BEZ235 on radiosensitivity. (**a**) RT can induce CaP-RR cells with EMT and enhanced CSC phenotypes, and activation of the PI3K/Akt/mTOR signaling pathway, resulting in CaP metastasis and recurrence after RT. (**b**) A dual PI3K/mTOR inhibitor BEZ235 combined with RT can inactivate the PI3K/Akt/mTOR signaling pathway, reducing EMT and CSC phenotypes and leading to increased radiosensitivity. All data used in RR cell lines were based on cells between 5 and 6 weeks post radiation treatment

enhances radiosensitivity in CaP cells, further confirming that targeting CSCs may overcome CaP radioresistance and prevent recurrence after RT. Our findings suggest that combination of RT with a CSC-targeted therapeutic strategy holds promise in the future CaP treatment.

Chk1 is a kinase that phosphorylates cdc25, an important phosphatase in cell cycle control, particularly for entry into mitosis. It was reported that Chk1 knockdown confers radiosensitization in CaP stem cells, suggesting that Chk1 has import role in CaP radioresistance and is associated with CSCs.[28] Chk2 is a protein kinase that is activated in response to DNA damage and is involved in cell cycle arrest.[29] Our results indicate that Chk1 and Chk2 were activated in CaP-RR cells compared with CaP-controls cells, suggesting that the activated Chk1/2 may be responsible for affecting cell cycle and DNA repair to provide time for cells to repair sublethal DNA damage which ensures cell survival.[16,30] The activation of Chk1 and Chk2 may be one of mechanisms for CaP radioresistance after RT.

As a major regulator of the PI3K/Akt/mTOR pathway, Akt is a serine/threonine protein kinase that has a critical role in suppressing apoptosis by regulating its downstream pathway and a target for radiosensitization. The mTOR acts as a downstream effector for Akt, and regulates key processes such as cell growth and proliferation, cell cycle progression and protein translation through two distinct pathways: one involving the ribosomal p70S6 kinase (p70S6K), and the other one involving eukaryotic translation initiation factor 4E (eIF4E)-binding proteins (4E-BPs).[31] In the current study, we found the phosphorylated-Akt, mTOR, S6K and 4EBP1 proteins (PI3K/Akt/mTOR signaling proteins) were significantly enhanced, whereas the total Akt, mTOR, S6K and 4EBP1 proteins were unchanged in CaP-RR cells compared with the CaP-control cells, suggesting that the PI3K/Akt/mTOR signaling pathway is activated in CaP-RR cells and that this pathway may have an important role in CaP radioresistance and be associated with the EMT and enhanced CSC phenotypes.

To further investigate the link between the activation of the PI3K/Akt/mTOR signaling pathway and EMT/CSC phenotypic change in CaP radioresistance, it needs to block this pathway to see how to affect the phenotypic expression of EMT/CSCs. Single PI3K/Akt/mTOR inhibitors (PI3K/Akt or mTOR inhibitors) combined with RT have been studied in several cancers. In this study, we chose a dual PI3K/mTOR inhibitor BEZ235 to investigate its effect on EMT/CSC phenotypes and radiosensitivity in CaP-RR cells. The reasons to use this dual inhibitor are that (1). Dual PI3K/mTOR inhibitors such as BEZ235 have many advantages over single inhibitors in cancer treatment;[32] (2). BEZ235 is a potent dual pan class I PI3K and mTOR inhibitor that inhibits the growth of CaP (PC-3) and other malignant cells in mouse xenograft models;[33] (3). BEZ235 has been used in a Phase I/II clinical trial for advanced breast cancer patients (NCT00620594) and is promising for future translational research in CaP clinical trials. After treatment with RT alone or combination with a low dose of BEZ235 and RT, we found that the combination treatment can reduce the expression of p-Akt, p-mTOR, p-S6K and p-4EBP1 as well as EMT/CSC phenotypes, at the same time, greatly increase radiosensitivity and induce more apoptosis compared with single RT or BEZ235 treatment or untreated control in CaP-RR cells. These results indicate that BEZ235 can greatly improve radiosensitivity and overcome radioresistance in CaP-RR cells through inhibiting the PI3K/Akt/mTOR signaling pathway associated with the down-regulation of EMT/CSC expression. Our findings further confirm that CaP radioresistance is associated with the EMT and enhanced CSCs phenotypes, activation of the PI3K/Akt/mTOR. Our results indicate that targeting the EMT, CSCs or PI3K/Akt/mTOR signaling pathway proteins holds promise in CaP RT.

In summary, we demonstrate for the first time that CaP radioresistance is associated with several mechanisms including EMT, CSCs, activation of the PI3K/Akt/mTOR signaling pathway and checkpoint proteins which result in cancer cell growth, survival, invasion, DNA repair and metastasis. Combination of a dual PI3K/Akt/mTOR pathway inhibitor (BEZ235) with RT can overcome CaP radioresistance and holds promise for future CaP treatment.

Materials and Methods

Antibodies and reagents. Antibodies were obtained from different sources. The detailed information and conditions for all antibodies are listed in Table 1. The BEZ235 dual inhibitor was obtained from Cayman Chemical, Co., Ann Arbor, MI, USA and was prepared as 1 mg/ml stock solution in chloroform, which was purged with argon and stored at $-20\,^\circ C$ for use.

Cell line and cell culture. The PC-3, DU145, LNCaP and RWPE-1 cell lines were obtained from American Type Culture Collection (ATCC) (Rockville, MD, USA). All tissue culture reagents were supplied by Invitrogen Australia Pty Ltd (Melbourne, VIC, Australia), unless otherwise stated. PC-3, DU145 and LNCaP cell lines were cultured in RPMI-1640 supplemented with 10% heated-inactivated fetal bovine serum (FBS), 50 U/ml of penicillin and 50 μg/ml of streptomycin. RWPE-1 cell line was cultured in Keratinocyte Serum-Free Medium (K-SFM) supplemented with 0.05 mg/ml bovine pituitary extract and 5 ng/ml human recombinant epidermal growth factor (EGF). All cell lines were maintained in a humidified incubator at 37 $^\circ C$ and 5% CO_2. The cells with 80–90% confluency were rinsed twice with Dulbecco's phosphate-buffered saline (DPBS) (pH7.2), detached with 0.25% trypsin/0.05% EDTA at 37 $^\circ C$, collected by centrifuge and resuspended in medium and followed by experiments.

Radiation for CaP cell lines. Flasks (75 cm^2) with 60% confluent cells were lying with a 1 cm thick compensation above and 100 cm source surface distance (SSD) below and the field size was 30 × 30 cm. PC-3, DU145 and LNCaP (4×10^6) cells were irradiated at the therapeutic radiation dosage of $\sim$2 Gy (226 mu) with 6 MV photons (Elekta, Stockholm, Sweden) for 5 consecutive days (Cancer Care Centre, St. George Hospital, Sydney, Australia) as a published method with some modifications.[34] Following the final radiation, the CaP cell lines were maintained as the above culture method in a humidified incubator at 37 $^\circ C$ and 5% CO_2 for $\sim$35 days for recovery. Non-irradiated controls were handled identically to the irradiate cells without radiation exposure.

Clonogenic survival assay. Radioresistance was measured by a clonogenic survival assay following exposure to irradiation. Briefly, 1500 cells were seeded in 10 cm dishes and were exposed to a range of radiation doses (2–10 Gy). The media were replaced regularly and all cultures were incubated for 14 days until the colonies were large enough to be clearly discerned. The positive colonies, defined as groups of >50 cells, were scored manually with the aid of an Olympus INT-2 inverted microscope (Tokyo, Japan). The survival fraction was calculated as the numbers of colonies divided by the numbers of cells seeded times plating efficiency. The average number of colonies were plotted (mean $\pm$ S.D., $n = 3$).

Matrigel invasion assay. Invasive ability of CaP-RR and CaP-control cells was determined using commercial matrigel and control transwell chambers (BD Bioscience, NSW, Australia). Briefly, 1.5×10^4 cells in 500 μl serum-free medium were added to each transwell insert and 750 μl complete medium was added to the outer well to provide chemoattractant and prevent dehydration. Cells were incubated at 37 $^\circ C$ in 5% CO_2 for 72 h and then stained with a Diff-Quik staining kit (Allegiance Healthcare Corp, McGraw Park, IL, USA). Excess dye was washed away with tap water and the number of stained cells that invaded through matrigel or control inserts was counted in five high-power fields (hpf) by light microscopy (Leica microscope, Nussloch, Germany). Invasive potential was calculated as follows: % Invasion = ((Mean cells invading through matrigel insert membrane)/(Mean cells migrating through control insert membrane)) × 100%. Cell invasion rates were plotted (Mean $\pm$ S.D., $n = 3$).

Sphere formation. Sphere formation assay was performed using a published method.[35] Briefly, CaP-RR and CaP-control cells were trypsinised, dissociated into single cells and then plated into an ultra low attachment round-bottom 96-well plates (Sigma-Aldrich Pty Ltd., Castle Hill, NSW, Australia). Final five cells in 100 μl serum-free DMEM/F12K media supplemented with 4 μg/ml insulin, B27 and 20 ng/ml EGF and bFGF were added into each well. Spheres that arose in 1 week were counted. The diameters of each sphere were observed and measured using an inverted phase microscope (CK-2, Olympus, Tokyo, Japan) fitted with an ocular eyepiece after 5 days. Sphere formation capacity was assessed as the number of spheres with the diameter of $>50\,\mu m$.

Immunofluorescent staining. Immunofluorescence staining was performed as previously described.[36] Briefly, CaP-RR and CaP-control cells were grown on glass coverslips (2×10^4 cells) for 24 h. After washing with Tris-buffered saline (TBS) (pH 7.5), the cells were fixed on coverslips in ice-cold methanol for 10 min at room temperature (RT) and then incubated with 10% normal goat serum in TBS for 20 min to suppress the nonspecific binding of IgG. The cells were then incubated with various primary antibodies (Table 1) overnight (o/n) at 4 $^\circ C$. After rinsing in TBS, cells were incubated for 45 min in Alexa Fluor-488 goat anti-mouse, Alexa Fluor-488 goat anti-rabbit or Alexa Fluor-488 Donkey anti-goat IgG (1 : 1000 dilutions) at RT. Propidium iodide (PI) (0.2 mg/l) was used to stain the nuclei. Negative controls were treated identically but omitted with the primary antibodies. Immunofluorescence was visualized using an FV 300/FV500 Olympus laser scanning confocal microscope (Olympus).

Western blotting analysis. Protein expression levels were determined by western blotting analysis as previously described.[37] Briefly, total proteins were extracted with RIPA buffer (Thermo Scientific, Rockford, IL, USA) and measured using a BCA kit (Thermo Scientific). Proteins were resolved on 4–20% Tris-Nupage gels (Invitrogen Australia Pty Ltd) and transferred to polyvinylidene fluoride membranes. Membranes were blocked in 5% bovine serum albumin (Sigma-Aldrich, Sydney, NSW, Australia) with 0.1% Tween-20 (PBST) for 1 h, and then incubated with different primary antibodies at 4 $^\circ C$ o/n (Table 1), followed by

Table 1 Antibodies used for immunofluorescence (IF) staining and western blot (WB)

Antibody	Source	Type	Dilution for WB and IF	Incubation time ($_{min}$)	Temperature	Application
Rabbit anti-human E-cadherin	Epitomics Inc.	MAb	1 : 2000 (WB) 1 : 500 (IF, IHC)	O/N	4 °C	WB, IF
Rabbit anti-human N-cadherin	Abcam	PAb	1 : 200 (WB) 1 : 200 (IF, IHC)	O/N	4 °C	WB, IF
Rabbit anti-human Vimentin	Epitomics Inc.	MAb	1 : 2000 (WB) 1 : 100 (IF, IHC)	O/N	4 °C	WB, IF
Rabbit anti-human OCT3/4	Epitomics Inc.	PAb	1 : 1000 (WB) 1 : 100 (IF, IHC)	O/N	4 °C	WB, IF
Rabbit anti-human SOX2	Epitomics Inc.	MAb	1 : 1000 (WB) 1 : 100 (IF, IHC)	O/N	4 °C	WB, IF
Rabbit anti-human alpha smooth muscle Actin	Abcam	PAb	1 : 1000 (WB) 1 : 100 (IF, IHC)	O/N	4 °C	WB, IF
Mouse anti-human CD44 (DF1485)	Santa Cruz Biotechnology	MAb	1 : 200 (WB, IF, IHC)	O/N	4 °C	WB, IF
Mouse anti-human CD44v6	Abcam	MAb	1 : 1000 (WB) 1 : 100 (IF, IHC)	O/N	4 °C	WB, IF
Rabbit anti-human CD326	Epitomics Inc.	PAb	1 : 1000 (WB) 1 : 100 (IF, IHC)	O/N	4 °C	WB, IF
Goat anti-human ALDH1A1	Santa Cruz Biotechnology	PAb	1 : 200 (WB, IF, IHC)	O/N	4 °C	WB, IF
Rabbit anti-human Nanog	Abcam	PAb	1 : 1000 (WB) 1 : 1000 (IF, IHC)	O/N	4 °C	WB, IF
Rabbit anti-human Snail	Abcam	PAb	1 : 500 (WB) 1 : 100 (IF, IHC)	O/N	4 °C	WB, IF
Rabbit anti-human Akt	Abcam	PAb	1 : 1000 (WB) 1 : 200 (IF, IHC)	O/N	4 °C	WB
Rabbit anti-human P-Akt	Abcam	PAb	1 : 1000 (WB) 1 : 200 (IF, IHC)	O/N	4 °C	WB
Rabbit anti-human mTOR	Cell Signaling	PAb	1 : 1000 (WB) 1 : 200 (IF, IHC)	O/N	4 °C	WB
Rabbit anti-human P-mTOR	Cell Signaling	PAb	1 : 1000 (WB) 1 : 200 (IF, IHC)	O/N	4 °C	WB
Rabbit anti-human S6k	Abcam	MAb	1 : 1000 (WB) 1 : 200 (IF, IHC)	O/N	4 °C	WB
Rabbit anti-human P-S6k	Abcam	PAb	1 : 1000 (WB) 1 : 200 (IF, IHC)	O/N	4 °C	WB
Rabbit anti-human 4EBP1	Cell Signaling	MAb	1 : 1000 (WB) 1 : 1600 (IF, IHC)	O/N	4 °C	WB
Rabbit anti-human P-4EBP1	Cell Signaling	MAb	1 : 1000 (WB) 1 : 200 (IF, IHC)	O/N	4 °C	WB
Mouse anti-human β-tubulin	Sigma	MAb	1 : 5000 (WB)	O/N	4 °C	WB
Mouse anti-GAPDH	Merck Millipore	PAb	1 : 2000 (WB)	O/N	4 °C	WB
Goat anti-rabbit IgG-HRP	Santa Cruz Biotechnology	IgG	1 : 5000 (WB)	45	RT	WB
Goat anti-mouse IgG-HRP	Santa Cruz Biotechnology	IgG	1 : 5000 (WB)	45	RT	WB
Donkey anti- Goat IgG-HRP	Santa Cruz Biotechnology	IgG	1 : 5000 (WB)	45	RT	WB
Goat anti-mouse Alexa Fluor 488 Dye Conjugate	Invitrogen	IgG	1 : 1000 (IF)	45	RT	IF
Goat anti-rabbit Alexa Fluor 488 Dye Conjugate	Invitrogen	IgG	1 : 1000 (IF)	45	RT	IF
Donkey anti- Goat Alexa Fluor 488 Dye Conjugate	Invitrogen	IgG	1 : 1000 (IF)	45	RT	IF

Abbreviations: HRP, horseradish peroxidase; MAb, monoclonal antibody; O/N, overnight; PAb, polyclonal antibody; RT, room temperature

incubation in horseradish peroxidase (HRP)-conjugated secondary antibodies (goat anti-mouse, goat anti-rabbit or donkey anti-goat appropriate for the host species of primary antibody) (1 : 2000 dilution). Immunoreactive bands were detected using enhanced chemiluminescence (ECL) substrate (Pierce Chemical Co, Rockford, IL, USA), and imaged using the ImageQuant LAS4000 system (GE Healthcare, Pittsburgh, PA, USA). To confirm equal loading of protein lysates, membranes were stripped (Restore Western Blot Stripping Buffer, Pierce, Rockford, IL, USA) and re-probed using mouse anti-β-tubulin monoclonal antibodies (MAb) (1 : 5000 dilution) or mouse anti-GAPDH polyclonal antibody (PAb) (1 : 2000 dilution), then processed as above. Images were processed in Adobe Photoshop.

Quantitative real-time PCR. Primers for EMT, CSCs and GAPDH (control) were synthesized (Invitrogen, Mulgrave, VIC, Australia). Total RNA was isolated using the RNAeasy kit (QIAGEN, Chadstone Centre, VIC, Australia) according to the manufacturer's instructions. Briefly, 1 μg of RNA from each CaP-RR and CaP-control cell line was reverse transcribed into cDNA using the SuperScript III Platinum Two-Step qRT-PCR Kit with SYBR Green (Invitrogen) following the manufacturer's instructions. After synthesis, samples were used for qPCR as in our published method.[16]

***In vitro* cell cytotoxicity assay.** Cell cytotoxicity was evaluated in CaP-RR and CaP-control cell lines as well as in normal prostate RWPE-1 cell line after BEZ235 treatment using MTT assay, following a published method.[17] Briefly, 2000 cells were seeded in 96-well plates incubated in culture media for 24 h. Cells were then treated with a range of concentrations of BEZ235 (0–1000 nM) or the same volume of DMSO control in fresh media for another 24 h, 48 h and 72 h, respectively. The absorbance (OD) was read at 560 nm on a BIO-TEC micro-plate reader (BIO-RAD, Hercules, CA, USA). Each experiment was repeated at least three times. Results are represented as the OD ratio of the treated and vehicle-

control cells. The ½ IC$_{50}$ values (50% inhibitory concentrations) of BEZ235 in CaP-RR cell lines at 24 h were calculated and chosen for the following experiments.

Radiosensitivity assay. To examine the effect of radiosensitivity by BEZ235, 1000 CaP-RR cells were seeded in each 10 cm^2 dish and incubated at 37 °C and 5% CO_2, in a humidified incubator and then treated with vehicle control or ½ IC$_{50}$ dose of BEZ235 for 24 h, or RT (6 Gy) for 12 h, or combination treatment (½ IC$_{50}$ dose of BEZ235 and 6 Gy radiation) for 24 h. For the combination treatment, the cultured cells were first treated with BEZ235 (½ IC$_{50}$) and after 12 h treatment, the treated cells were exposed to 6 Gy radiation and then combination of BEZ235 and RT for another 12 h. The single dose (6 Gy) irradiation was performed using a linear accelerator (Elekta, Stockholm, Sweden) at a dose rate of 2.7 Gy/min with 6 MV photons (Cancer Care Centre). The colony formation assay was performed as above. The average numbers of colonies were plotted (Mean ± S.D., $n = 3$).

Detection of apoptosis. PC-3RR, DU145RR and LNCaPRR cells (5 × 10^5) were cultured in 25 cm^2 flasks for 24 h and then treated with vehicle control, ½ IC$_{50}$ BEZ235, single RT (6 Gy), or combination treatment with ½ IC$_{50}$ BEZ235 and RT (6 Gy). Cells exposed to different treatments were then stained with the DNA-binding agents AO/EB (Sigma-Aldrich Pty Ltd) as previously published method[17] and examined with confocal microscopy (FV 300/FV500 Olympus). Apoptotic cells were characterized by morphology including nuclear condensation and fragmentation.

Assessment of immunostaining results. Staining intensity (0–3) in CaP cell lines was assessed using a confocal microscope (Olympus). The criteria used for assessment were as previously reported,[36] where: 0 (negative, 25%); 1 + (weak, 25–50%); 2 + (moderate, 50–70%); 3 + (strong, 75%) of the tumor cells stained. Evaluation of cell staining was performed, independently, by three

experienced observers (LC, JLH and YL). All slides were scored blind and an average of grades was taken.

Statistical analysis. All experiments were performed at least three times ($n = 3$). All numerical data were expressed as the average of the values (Mean), and the standard deviation (S.D.) was calculated. For irradiation experiments, survival fractions were calculated as mean plating efficiency of radiation-treated cells/mean plating efficiency of control cells $\times$ 100%.[16] RT survival curves were fitted according to the linear-quadratic model using GraphPad Prism 4.0 software (GraphPad, San Diego, CA, USA): $Survival = e^{-(\alpha D + \beta D^2)}$. Possible significant differences ($P < 0.05$) were evaluated using SPSS v16.0 software (SPSS, Chicago, IL, USA).

Conflict of Interest

The authors declare no conflict of interest.

1. Beltran H, Beer TM, Carducci MA, de Bono J, Gleave M, Hussain M et al. New therapies for castration-resistant prostate cancer: efficacy and safety. Eur Urol 2011; 60: 279–290.
2. Jemal A, Siegel R, Xu J, Ward E. Cancer statistics 2010. CA Cancer J Clin 2010; 60: 277–300.
3. Khan MA, Walsh PC, Miller MC, Bales WD, Epstein JI, Mangold LA et al. Quantitative alterations in nuclear structure predict prostate carcinoma distant metastasis and death in men with biochemical recurrence after radical prostatectomy. Cancer 2003; 98: 2583–2591.
4. Eade TN, Hanlon AL, Horwitz EM, Buyyounouski MK, Hanks GE, Pollack A. What dose of external-beam radiation is high enough for prostate cancer? Int J Radiat Oncol Biol Phys 2007; 68: 682–689.
5. Coen JJ, Bae K, Zietman AL, Patel B, Shipley WU, Slater JD et al. Acute and late toxicity after dose escalation to 82 GyE using conformal proton radiation for localized prostate cancer: initial report of American College of Radiology Phase II study 03-12. Int J Radiat Oncol Biol Phys 2011; 81: 1005–1009.
6. Leith JT. In vitro radiation sensitivity of the LNCaP prostatic tumor cell line. Prostate 1994; 24: 119–124.
7. Zhou YC, Liu JY, Li J, Zhang J, Xu YQ, Zhang HW et al. Ionizing radiation promotes migration and invasion of cancer cells through transforming growth factor-beta-mediated epithelial-mesenchymal transition. Int J Radiat Oncol Biol Phys 2011; 81: 1530–1537.
8. Hay ED. The mesenchymal cell, its role in the embryo, and the remarkable signaling mechanisms that create it. Dev Dyn 2005; 233: 706–720.
9. Kong D, Li Y, Wang Z, Sarkar FH. Cancer Stem cells and epithelial-to-mesenchymal transition (emt)-phenotypic cells: are they cousins or twins? Cancers (Basel) 2011; 3: 716–729.
10. Sarkar FH, Li Y, Wang Z, Kong D. The role of nutraceuticals in the regulation of Wnt and Hedgehog signaling in cancer. Cancer Metastasis Rev 2010; 29: 383–394.
11. Singh A, EMT Settleman J. cancer stem cells and drug resistance: an emerging axis of evil in the war on cancer. Oncogene 2010; 29: 4741–4751.
12. Josson S, Sharp S, Sung SY, Johnstone PA, Aneja R, Wang R et al. Tumor-Stromal Interactions influence radiation sensitivity in epithelial- versus mesenchymal-like prostate cancer cells. J Oncol 2010; 2010: Article ID 232831, doi:10.1155/2010/232831.
13. Tiwari N, Gheldof A, Tatari M, Christofori G. EMT as the ultimate survival mechanism of cancer cells. Semin Cancer Biol 2012; 22: 194–207.
14. Yu C, Shiozawa Y, Taichman RS, McCauley LK, Pienta K, Keller E. Prostate cancer and parasitism of the bone hematopoietic stem cell niche. Crit Rev Eukaryot Gene Expr 2012; 22: 131–148.
15. Bao S, Wu Q, McLendon RE, Hao Y, Shi Q, Hjelmeland AB et al. Glioma stem cells promote radioresistance by preferential activation of the DNA damage response. Nature 2006; 444: 756–760.
16. Xiao W, Graham PH, Power CA, Hao J, Kearsley JH, Li Y. CD44 is a biomarker associated with human prostate cancer radiation sensitivity. Clin Exp Metastasis 2012; 29: 1–9.
17. Chao H, Wang L, Hao J, Ni J, Chang L, Graham PH et al. Low dose histone deacetylase inhibitor, LBH589, potentiates anticancer effect of docetaxel in epithelial ovarian cancer via PI3K/Akt pathway in vitro. Cancer Lett 2013; 329: 17–26.
18. Jung P, Sato T, Merlos-Suarez A, Barriga FM, Iglesias M, Rossell D et al. Isolation and in vitro expansion of human colonic stem cells. Nat Med 2011; 17: 1225–1227.
19. Fillmore CM, Kuperwasser C. Human breast cancer cell lines contain stem-like cells that self-renew, give rise to phenotypically diverse progeny and survive chemotherapy. Breast Cancer Res 2008; 10: R25.
20. Ansieau S, Bastid J, Doreau A, Morel AP, Bouchet BP, Thomas C et al. Induction of EMT by twist proteins as a collateral effect of tumor-promoting inactivation of premature senescence. Cancer Cell 2008; 14: 79–89.
21. Mani SA, Guo W, Liao MJ, Eaton EN, Ayyanan A, Zhou AY et al. The epithelial-mesenchymal transition generates cells with properties of stem cells. Cell 2008; 133: 704–715.
22. Nishida S, Hirohashi Y, Torigoe T, Kitamura H, Takahashi A, Masumori N et al. Gene expression profiles of prostate cancer stem cells isolated by aldehyde dehydrogenase activity assay. J Urol 2012; 188: 294–299.
23. Ni J, Cozzi PJ, Duan W, Shigdar S, Graham PH, John KH et al. Role of the EpCAM (CD326) in prostate cancer metastasis and progression. Cancer Metastasis Rev 2012; 31: 779–791.
24. Hao JLNJ, Graham P, Cozzi PJ, Bucci J, Kearsley J et al. The CD44 isoforms in prostate cancer metastasis and progression. World J.Cancer Res 2013; 1: 3–14.
25. Noh KH, Kim BW, Song KH, Cho H, Lee YH, Kim JH et al. Nanog signaling in cancer promotes stem-like phenotype and immune evasion. J Clin Invest 2012; 122: 4077–4093.
26. Zhu LF, Hu Y, Yang CC, Xu XH, Ning TY, Wang ZL et al. Snail overexpression induces an epithelial to mesenchymal transition and cancer stem cell-like properties in SCC9 cells. Lab Invest 2012; 92: 744–752.
27. Jeter CR, Liu B, Liu X, Chen X, Liu C, Calhoun-Davis T et al. NANOG promotes cancer stem cell characteristics and prostate cancer resistance to androgen deprivation. Oncogene 2011; 30: 3833–3845.
28. Wang X, Ma Z, Xiao Z, Liu H, Dou Z, Feng X et al. Chk1 knockdown confers radiosensitization in prostate cancer stem cells. Oncol Rep 2012; 28: 2247–2254.
29. Matsuoka S, Huang M, Elledge SJ. Linkage of ATM to cell cycle regulation by the Chk2 protein kinase. Science 1998; 282: 1893–1897.
30. Gogineni VR, Nalla AK, Gupta R, Dinh DH, Klopfenstein JD, Rao JS. Chk2-mediated G2/M cell cycle arrest maintains radiation resistance in malignant meningioma cells. Cancer Lett 2011; 313: 64–75.
31. Chang L, Graham PH, Hao JL, Bucci J, Cozzi PJ, Kearsley JK et al. Emerging roles of radioresistance in prostate cancer metastasis and radiation therapy. Cancer Metast Rev 2013; In press.
32. Chen J. Potential value and limitation of dual inhibitors of PI3K and mTOR in the treatment of cancer. Curr Cancer Drug Targets 2013; 13: 117–120.
33. Maira SM, Stauffer F, Brueggen J, Furet P, Schnell C, Fritsch C et al. Identification and characterization of NVP-BEZ235, a new orally available dual phosphatidylinositol 3-kinase/mammalian target of rapamycin inhibitor with potent in vivo antitumor activity. Mol Cancer Ther 2008; 7: 1851–1863.
34. Smith L, Qutob O, Watson MB, Beavis AW, Potts D, Welham KJ et al. Proteomic identification of putative biomarkers of radiotherapy resistance: a possible role for the 26S proteasome? Neoplasia 2009; 11: 1194–1207.
35. Della Donna L, Lagadec C, Pajonk F. Radioresistance of prostate cancer cells with low proteasome activity. Prostate 2012; 72: 868–874.
36. Wang L, Chen H, Liu F, Madigan MC, Power CA, Hao J et al. Monoclonal antibody targeting MUC1 and increasing sensitivity to docetaxel as a novel strategy in treating human epithelial ovarian cancer. Cancer Lett 2011; 300: 122–133.
37. Hao J, Madigan MC, Khatri A, Power CA, Hung TT, Beretov J et al. In vitro and in vivo prostate cancer metastasis and chemoresistance can be modulated by expression of either CD44 or CD147. PLoS One 2012; 7: e40716.

Supplementary Information accompanies this paper on Cell Death and Disease website (http://www.nature.com/cddis)